Transcriptional heterogeneity and tightly regulated changes in gene expression during *Plasmodium berghei* sporozoite development

Haikel N. Bogale[a], Tales V. Pascini[b], Sachie Kanatani[c], Juliana M. Sá[b], Thomas E. Wellems[b,1], Photini Sinnis[c], Joel Vega-Rodríguez[b], and David Serre[a,d,1]

[a]Institute for Genome Sciences, University of Maryland School of Medicine, Baltimore, MD 21201; [b]Laboratory of Malaria and Vector Research, National Institute of Allergy and Infectious Diseases, National Institutes of Health, Bethesda, MD 20892; [c]Department of Molecular Microbiology and Immunology, Johns Hopkins Bloomberg School of Public Health, Baltimore, MD 21205; and [d]Department of Microbiology and Immunology, University of Maryland School of Medicine, Baltimore, MD 21201

Contributed by Thomas E. Wellems, January 18, 2021 (sent for review November 11, 2020; reviewed by Daniel E. Neafsey and Ashley M. Vaughan)

Despite the critical role of *Plasmodium* sporozoites in malaria transmission, we still know little about the mechanisms underlying their development in mosquitoes. Here, we use single-cell RNA sequencing to characterize the gene expression profiles of 16,038 *Plasmodium berghei* sporozoites isolated throughout their development from midgut oocysts to salivary glands, and from forced salivation experiments. Our results reveal a succession of tightly regulated changes in gene expression occurring during the maturation of sporozoites and highlight candidate genes that could play important roles in oocyst egress, sporozoite motility, and the mechanisms underlying the invasion of mosquito salivary glands and mammalian hepatocytes. In addition, the single-cell data reveal extensive transcriptional heterogeneity among parasites isolated from the same anatomical site, suggesting that *Plasmodium* development in mosquitoes is asynchronous and regulated by intrinsic as well as environmental factors. Finally, our analyses show a decrease in transcriptional activity preceding the translational repression observed in mature sporozoites and associated with their quiescent state in salivary glands, followed by a rapid reactivation of the transcriptional machinery immediately upon salivation.

malaria | single-cell analysis | gene expression

Malaria is a disease caused by unicellular parasites of the *Plasmodium* genus that are transmitted to humans by the bites of infected female *Anopheles* mosquitoes. Socioeconomic development (1–4), combined with the use of extensive entomological controls (5, 6) and improved antimalarial drug development and distribution (7, 8), have significantly decreased the mortality associated with malaria over the last 50 y. However, the disease remains a heavy burden affecting more than 200 million people and responsible for half a million deaths annually (9). An efficient malaria vaccine remains elusive, but encouraging progress has been achieved in recent years with the development and testing of vaccines using recombinant proteins (10, 11) and attenuated parasites (12–14) from the human infective stage, the sporozoite. However, despite renewed interest in *Plasmodium* mosquito stages for vaccine development, many of the molecular processes regulating sporozoite development remain unclear.

Following the ingestion of male and female gametocytes during a blood feeding, fertilization occurs in the mosquito midgut, producing zygotes that undergo meiosis and develop into motile ookinetes. The ookinete traverses the midgut epithelium and matures into an oocyst. On the basal surface of the midgut epithelium, the sessile oocyst undergoes multiple cycles of DNA replication and cell divisions, which leads to the production of thousands of sporozoites that are released into the mosquito's hemolymph. The crescent-shaped sporozoites are then transported by the hemolymph and ~20% of them successfully enter the salivary glands, where they wait to be inoculated into a mammalian host, remaining viable for days to weeks (15). Transmission to the mammalian host occurs when a small number of sporozoites, typically less than 100, are ejected with the mosquito saliva into the dermis during the probing phase of a bite (16, 17). Once in the skin, sporozoites move rapidly to locate blood vessels and enter the blood circulation, which carries them to the liver, where they enter hepatocytes and develop into liver stages. During their migration, from the mosquito midgut to the mammalian liver, sporozoites do not show major morphological changes but go through important developmental changes. For example, sporozoites collected from oocysts or from the hemolymph can cause successful mammalian infections but these sporozoites are, overall, much less infectious than salivary gland sporozoites (18–20). Conversely, sporozoites collected from a salivary gland and injected into the hemolymph show reduced infectivity for the mosquito salivary glands (21). These changes in infectivity are mirrored by changes in mRNA expression and protein abundance that have been characterized for rodent parasites and, to a lesser extent, for *Plasmodium falciparum* (22, 23). Combined with elegant reverse genetic experiments, these analyses have highlighted some of the molecular processes underlying sporozoite maturation, and revealed key *Plasmodium* genes involved in sporozoite egress from the oocyst [e.g., PbSERA5 (24), SIAP-1 (25), and PCRMPs (26)], and in the

Significance

A better understanding of the molecular mechanisms underlying the development of *Plasmodium* parasites in *Anopheles* mosquitoes would facilitate the development of malaria vaccines and of novel strategies to interrupt disease transmission. We characterized, at the single-cell level, the gene expression profiles of sporozoites from the rodent malaria parasite *Plasmodium berghei*, throughout their development in mosquitoes and upon salivation. Our analyses reveal heterogeneity in gene expression among parasites isolated from the same anatomical location, suggesting that parasite development is asynchronous in mosquitoes. In addition, our results highlight the role of gene expression changes in regulating the ability of sporozoites to remain quiescent in the salivary glands, and their rapid reactivation upon salivation.

Author contributions: J.M.S., T.E.W., P.S., J.V.-R., and D.S. designed research; H.N.B., T.V.P., S.K., and J.M.S. performed research; T.E.W., P.S., and J.V.-R. contributed new reagents/analytic tools; H.N.B., P.S., J.V.-R., and D.S. analyzed data; and H.N.B., T.E.W., P.S., J.V.-R., and D.S. wrote the paper.

Reviewers: D.E.N., Harvard University; and A.M.V., Seattle Children's Research Institute.

The authors declare no competing interest.

[1]To whom correspondence may be addressed. Email: twellems@niaid.nih.gov or dserre@som.umaryland.edu.

This article contains supporting information online at https://www.pnas.org/lookup/suppl/doi:10.1073/pnas.2023438118/-/DCSupplemental.

Published March 02, 2021.

recognition and invasion of the mosquito salivary glands [e.g., TREP (27), MAEBL (28), and CSP (29)]. However, despite these important studies, several outstanding questions remain regarding the regulation and development of *Plasmodium* sporozoites in mosquitoes. For example, it is not clear whether the maturation of sporozoites is primarily driven by extrinsic (e.g., the location of the sporozoites in the mosquito) or intrinsic factors (e.g., the age of the sporozoites) as these parameters are confounded in most studies. Similarly, we do not know whether all sporozoites at the same anatomical location are identically regulated or whether they mature asynchronously. These questions have been difficult to rigorously address due to technical limitations of available methods. In order to have sufficient amounts of material for analysis, genomic and proteomic studies typically rely on bulk approaches utilizing large numbers of parasites, which only provide "averages" on these populations and mask potential heterogeneity among individual parasites. The advent of single-cell technologies allows us to examine the regulation of individual cells and has already provided exciting new insights on the biology of *Plasmodium* parasites (30–33). Here, we use the rodent malaria parasite *Plasmodium berghei*, a parasite extensively used for studying preerythrocytic stages in the mammalian host and for performing forward genetic screens (34–36), to describe the transcriptomes of 16,038 individual sporozoites collected throughout their development, from oocysts to salivary glands, and salivated sporozoites, and analyze the succession of molecular changes, and their variations, occurring during these transitions.

Results and Discussion

Gene Expression Profiling of Individual *Plasmodium* Sporozoites. We analyzed *P. berghei* sporozoites collected throughout their development in *Anopheles stephensi* mosquitoes, from late-stage oocysts (14 d postinfection [dpi]), mosquito hemolymph (16 dpi), salivary glands (21 to 22 dpi), and forced salivation experiments (21 to 22 dpi) (Fig. 1*A*). Overall, these sporozoites were derived from a total of 12 independent collections, represented two *P. berghei* lines, and were isolated from two different *An. stephensi* colonies (*SI Appendix*, Table S1 and see *Materials and Methods* for details).

From each sample, we prepared a 3′-end 10× Genomics single-cell RNA-sequencing (scRNA-seq) library (37) and sequenced 128 to 248 million paired-end reads of 75 base pairs (*SI Appendix*, Table S1). Between 0.6 and 67.2% of the reads mapped to the *P. berghei* ANKA genome (38), providing, on average, 20.2 million *Plasmodium* reads per sample. Most of the remaining reads mapped to the *An. stephensi* genome and represented contamination by mosquito RNA. After stringent quality filters (*Materials and Methods*), we obtained between 82 and 4,630 single *Plasmodium* cell transcriptomes from each library, for a total of 16,038 individual sporozoite transcriptomes, each characterized by an average of 1,033 unique reads per parasite (235 to 5,867) (*SI Appendix*, Table S1).

scRNA-Seq Reveals Heterogeneous and Overlapping Changes in Gene Expression during *P. berghei* Sporozoite Development. We characterized the transcriptomes of 16,038 sporozoites: 614 sporozoites collected from disrupted oocysts, 2,147 sporozoites isolated from the mosquito hemolymph, 5,979 sporozoites dissected from mosquitoes' salivary glands, and 7,298 sporozoites obtained after forced salivation experiments (*SI Appendix*, Table S1). After excluding the transcripts of genes detected in less than 300 cells, we obtained expression data from 1,763 genes (out of the 5,120 protein-coding genes annotated in the *P. berghei* genome) for further analysis (*Materials and Methods*). To examine transcriptomic changes occurring during sporozoite development, we first compared, using principal component analysis (PCA), the gene expression profiles of individual sporozoites from different anatomical sites. Interestingly, while *P. berghei* sporozoites primarily clustered according to the anatomical site from which they were collected, the gene expression profiles showed extensive variations within, and overlap between, sporozoites isolated from different anatomical sites (Fig. 1*B*). For example, the gene expression profiles of hemolymph sporozoites (in blue on Fig. 1*B*) ranged from profiles indistinguishable from those of oocyst sporozoites (in red) to profiles similar to those of salivary gland sporozoites (in green), consistent with the range of phenotypes observed in this population.

To further examine changes in gene expression during *P. berghei* sporozoite development, while accounting for the apparent heterogeneity of each sample, we estimated the position of each individual sporozoite along a putative developmental trajectory (pseudotime) calculated solely using the gene expression data (39).

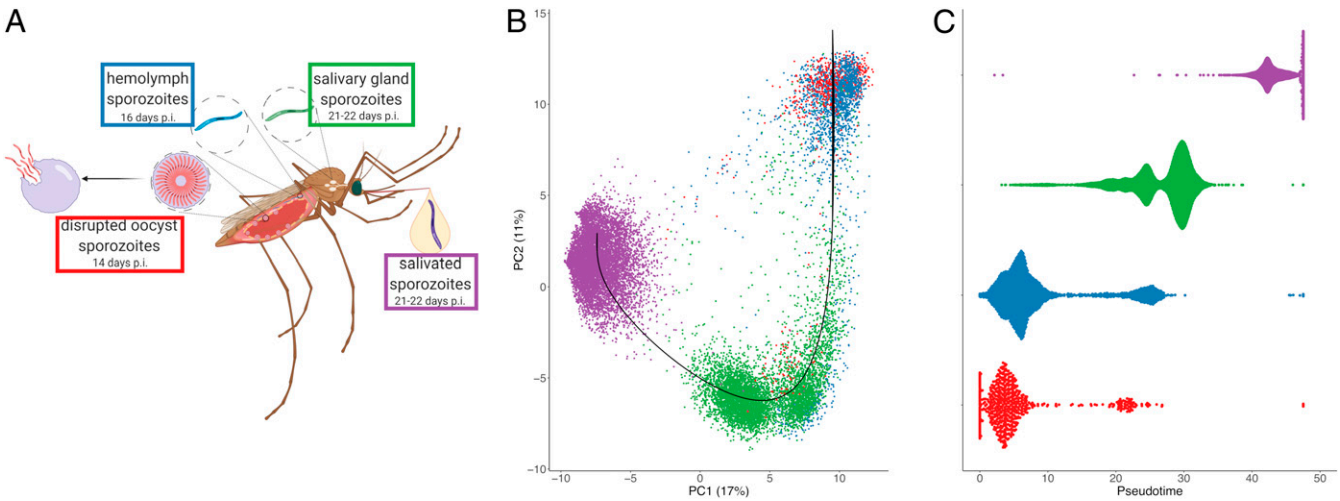

Fig. 1. Changes in gene expression during sporozoite development. (*A*) Schematic summarizing sporozoite populations included in this study and their time of collection in days postinfection (figure created with BioRender.com). (*B*) PCA showing the relationships among individual *P. berghei* sporozoites based on their expression profiles. Each dot represents a single sporozoite and is colored according to its collection site (red, disrupted oocysts; blue, hemolymph; green, salivary glands; purple, forced salivation). The black line shows the trajectory of the developmental pseudotime inferred based on the gene expression profiles. (*C*) Distribution of the pseudotime values (*x* axis) inferred for each individual sporozoite (each represented by a dot colored as in *B*) according to their collection site (*y* axis). Note the overlap between the distributions of each group.

This unsupervised analysis sequentially organized sporozoites starting with those collected from disrupted oocysts and ending with salivated sporozoites, but with significant overlaps between sporozoites collected at different points of their development (with the possible exception of salivated sporozoites that displayed a more distinct gene expression profile) (Fig. 1*C*). Some of this transcriptional heterogeneity could be accounted for by slight differences between biological replicates (*SI Appendix*, Fig. S1). In particular, we observed a shift between the modes of the distributions obtained from mCherry- and GFP-labeled salivary gland sporozoites, which could be due to differences in the times of collection or in the insectary temperatures, or the effect of the fluorophore and/or its level of expression in these genetically modified parasites. However, variations between replicates did not entirely explain the wide range of transcriptional heterogeneity observed among sporozoites collected at the same anatomical site, as distinct gene expression profiles were consistently observed within each biological replicate (*SI Appendix*, Fig. S1). Furthermore, to evaluate whether the "outlier cells" might represent technical artifacts caused by low signal, we repeated the analysis considering only cells characterized by more than 1,000 unique reads. The gene expression patterns observed were qualitatively similar to those from the entire dataset and confirmed high heterogeneity among sporozoites collected at the same site as well as overlaps between those collected at different sites (*SI Appendix*, Fig. S2).

Taken together, these analyses supported previous findings from microarray and RNA-seq studies that showed that gene expression changes over the course of sporozoite development (22, 23, 40), resulting in differences between parasites collected from different anatomical locations (since those were also correlated with the time postinfection; Fig. 1). However, the analysis of individual parasites enabled identifying heterogeneity among sporozoites at the same location, which was previously masked in bulk analyses. This heterogeneity could derive from differences in the rate of oocyst maturation and the time since sporozoite egress: *P. berghei* oocysts, within the same mosquito, develop asynchronously and can reach maturity at different times (41). It is therefore possible that the differences in gene expression observed among sporozoites reflect variations in their time since egress. Alternatively, these findings could indicate that the rate of sporozoite development stochastically varied between individual parasites, resulting in similar gene expression profiles between, for example, fast maturing sporozoites in the hemolymph and slower maturing salivary gland parasites. Finally, this analysis relied on parasites collected from multiple mosquitoes (*SI Appendix*, Table S1), which could account for some of the transcriptional heterogeneity: While each experiment used mosquitoes from the same colony and of the same age, it is possible that mosquito-specific factors influenced the rate of *Plasmodium* development and that the sporozoites with unusual transcriptional profiles (either delayed or accelerated) all derive from the same mosquito. Irrespective of the underlying reason for the transcriptional heterogeneity, the overlap observed between the gene expression profiles of sporozoites collected at different sites clearly indicated that *Plasmodium* development in the mosquito is not solely regulated by signals from their tissue environment: A small fraction of the oocyst and hemolymph sporozoites looked identical, transcriptionally, to salivary gland sporozoites suggesting that the development of the parasites does not entirely depend upon their anatomical location. This observation could explain why a few sporozoites collected from oocysts or hemolymph can induce mammalian infections (18–20): These successful infections would be caused by the minority of oocyst or hemolymph sporozoites with advanced maturation (i.e., those with greater pseudotimes on Fig. 1*C*).

Tightly Regulated Changes in Gene Expression during Sporozoite Development. To systematically identify genes differentially expressed during sporozoite development, we tested, for each individual *P. berghei* gene, whether the expression level was significantly associated with the developmental pseudotime, from oocyst to salivary gland sporozoites. Since salivated sporozoites displayed low mRNA abundance compared to sporozoites collected from other anatomical sites (see below), we excluded these parasites from the differential analysis reported here (but the results using all parasites are shown in Dataset S1 and *SI Appendix*, Fig. S3). This differential gene expression analysis recapitulated much of our current knowledge of sporozoite biology. Many genes with validated roles in oocyst egress and gliding motility [SSP3 (42)], salivary gland invasion [MAEBL (28), SIAP-1 (25), TREP (27), ICP (43)] or skin passage and development in the liver [UIS4 (44), UIS3 (45), CelTOS (46), UIS2 (47), TRSP (48), GEST (49), PL (50)] were among the most differentially expressed genes and displayed a timing of expression consistent with their known function (Table 1 and Fig. 2). CSP (51) and TRAP (52) showed high and sustained level of expression from oocyst to salivary gland sporozoites, consistent with previous reports (see, e.g., ref. 40), before decreases in their expression (discussed below). In addition to the information on these well-characterized genes, our analysis highlighted the potential role of genes not previously known to be important in sporozoites: For example, Plasmepsin X (PM-X, PBANKA_1222500), which has been shown to be involved in merozoite egress (53), was highly expressed during early sporozoite development, suggesting a possible role in oocyst egress, while bergheilysin (PBANKA_1137000) was expressed later, consistent with a putative role in salivary gland invasion or skin passage (Fig. 3*A*). Similarly, several genes without functional annotation or predicted domains showed high level of expression and tightly regulated timing of expression (Fig. 3*B*) consistent with a role in sporozoite development, and it will be exciting to further examine these potential candidates with functional studies. Finally, four AP2 domain transcription factor genes were consistently detected in the scRNA-seq data, including PBANKA_0521700, which was specifically expressed in salivary gland sporozoites (*SI Appendix*, Fig. S4). The complete list of genes is available in Dataset S1.

Despite the clear separation of salivated and salivary gland sporozoites based on their overall gene expression profiles (Fig. 1), few protein-coding genes were consistently transcribed in salivated sporozoites (*SI Appendix*, Table S2 and discussion below). Two notable exceptions were the early transcribed membrane protein (UIS4, PBANKA_0501200), which reached even higher levels of expression in salivated sporozoites than those observed in salivary gland sporozoites (*SI Appendix*, Fig. S5*A*), and an uncharacterized exported protein (PBANKA_1465051; *SI Appendix*, Fig. S5*B*), which contains a predicted circumsporozoite-related antigen domain and would be fascinating to functionally evaluate.

Transcription and Translation Are Dynamically Regulated in Sporozoites. Once they reach the salivary glands, *Plasmodium* sporozoites can remain quiescent for several days to weeks (15) before being injected into the mammalian host, where they quickly become motile and able to invade host cells (54). A proposed molecular mechanism underlying this quiescent state of salivary gland sporozoites and their rapid reactivation upon salivation is translational repression of the mRNAs encoding the proteins required later in the mammalian host (23, 55–57). This global translational repression results from the phosphorylation of the eukaryotic translation initiation factor 2-alpha by eIK2 (PBANKA_0205800) (55), while the Pumilio protein (PUF2, PBANKA_0719200) binds to the matching phosphatase-encoding transcripts (UIS2, PBANKA_1328000) and blocks their translation (reviewed in refs. 56, 58, and 59). Consistent with this mechanism, we observed a clear peak of expression of eIK2 and PUF2 in salivary gland sporozoites (Fig. 4*A*) but not in oocyst sporozoites, as has recently been described (23).

Some of the proteins regulating the long-term storage of the mRNAs in stress granules in female gametocytes have been characterized (e.g., refs. 57 and 60), but these genes do not seem to play

Table 1. List of the 30 genes most differentially expressed according to the sporozoite developmental pseudotime, from oocyst to salivary gland sporozoites

Gene	Annotation	Name	Max expr.	Phenotype (reference)	RMgmDB
PBANKA_1002500	Sporozoite-specific protein S10	S10	8	Liver [Togiri et al. (79)]	SG sporozoites (RMgm-2710)
PBANKA_0901300	Membrane associated erythrocyte binding-like protein	MAEBL	5	SG [Kariu et al. (28)]	SG sporozoites (RMgm-220)
PBANKA_0501200	Early transcribed membrane protein	UIS4	30+	Liver [Mueller et al. (44)]	Liver (RMgm-1934)
PBANKA_1465051	*Plasmodium* exported protein		30+		
PBANKA_1400800	Protein UIS3	UIS3	30	Liver [Mueller et al. (45)]	Liver (RMgm-1449)
PBANKA_1206800	Zinc finger (CCCH type) protein		8		No phenotype (RMgm-374, -3195)
PBANKA_1236200	Conserved *Plasmodium* protein		10		
PBANKA_1349800	Thrombospondin-related anonymous protein	TRAP	Sustained	Motility [Sultan et al. (52)]	SG sporozoites (RMgm-149, -1344)
PBANKA_1433700	Conserved *Plasmodium* protein		5		Egress (RMgm-312)
PBANKA_1425200	Sporozoite surface protein 3	SSP3	20	Motility [Harupa et al. (42)]	No phenotype (RMgm-3858)
PBANKA_1432300	Cell traversal protein for ookinetes and sporozoites	CelTOS	25	Skin plus liver [Kariu et al. (46)]	Oocysts (RMgm-46)
PBANKA_1006200	Sporozoite invasion-associated protein 1	SIAP1	Sustained	SG [Engelmann et al. (25)]	Egress (RMgm-109, -233)
PBANKA_1349300	Conserved *Plasmodium* protein		25		
PBANKA_1225000	Serine/threonine protein kinase, FIKK family		8	Oocysts [Jaiyan et al. (80)]	No data (RMgm-3295)
PBANKA_1236100	Ribosomal large subunit pseudouridylate synthase		10		
PBANKA_1340100	L-Lactate dehydrogenase	LDH	5		
PBANKA_1204200	IMP1-like protein	IMP4	0		No data (RMgm-3185)
PBANKA_1422900	Conserved protein		0		
PBANKA_0605900	Conserved *Plasmodium* protein		20		
PBANKA_1306500	TRAP-like protein	TREP	0	Motility [Combe et al. (27)]	SG sporozoites (RMgm-145, -159)
PBANKA_1328000	Serine/threonine protein phosphatase UIS2	UIS2	25	Liver [Zhang et al. (47)]	Liver (RMgm-1366)
PBANKA_0209100	Thrombospondin-related sporozoite protein	TRSP	20	Liver [Labaied et al. (48)]	Liver (RMgm-34)
PBANKA_0813000	Inhibitor of cysteine proteases	ICP	8, 25	SG [Boysen et al. (43)], liver [Lehmann et al. (81)]	SG sporozoites (RMgm-1114, -970)
PBANKA_1350500	Parasitophorous vacuolar prot. 3	PV3	8		
PBANKA_1312700	Gamete egress and sporozoite traversal protein	GEST	20	Skin [Talman et al. (49)]	Liver (RMgm-667)
PBANKA_0601600	Nuclear export mediator factor	NEMF	18		
PBANKA_0403200	Circumsporozoite (CS) protein	CSP	Sustained	Sporozoite development [Menard et al. (82)]	Sporozoites (RMgm-9)
PBANKA_1005200	Conserved *Plasmodium* protein		18		Liver (RMgm-2722)
PBANKA_0720800	RNA-binding protein NOB1	NOB1	5		
PBANKA_1107700	SET domain protein	SET9	5		

For each gene, the table indicates the gene name and annotation, the time of the peak of expression (Max Expr., in pseudotime units), whether the gene has been associated with a sporozoite phenotype in the literature (and the corresponding reference), and whether a phenotype is reported in the Rodent Malaria genetically modified Parasites database (RMgmDB). The genes are ranked based on the statistical significance of the association between expression and pseudotime (most significant on top). See *SI Appendix*, Table S2 for the complete list of genes, the statistical significance, and the results of the association when salivated sporozoites are included in the analysis).

a similar role in sporozoites. Indeed, aside from eIK2 and PUF2, none of the proteins involved in translational repression in gametocytes [e.g., DOZI or CITH (61)], nor the orthologous proteins of those associated with stress granules in humans or yeasts (62), were detectable in our dataset. Only the sporozoite asparagine-rich protein 1 (SAP-1), which has been shown to regulate mRNA stability in sporozoites (63, 64), was robustly detected and showed a pattern of expression akin to those of eIK2 and PUF2, although with an earlier peak of expression (Fig. 4*A*). Interestingly, among the genes expressed at the same time as eIK2, we observed one RNA helicase (PBANKA_1103800) that was lowly but specifically expressed in salivary gland sporozoites, and it will be interesting to test whether it may play a role in translational repression.

Finally, the increased expression of genes involved in translational repression appeared to be preceded by an overall and steady decrease in mRNA transcription (Fig. 4*B*). Fluctuations in overall mRNA abundance have been described in blood-stage *Plasmodium* parasites (65, 66), and the decrease in mRNA transcription during sporozoite development is consistent with the hypothesis that mature salivary gland sporozoites are quiescent and their transcriptional activity reduced. Conversely, we observed a twofold to threefold increase in the number of ribosomal RNA

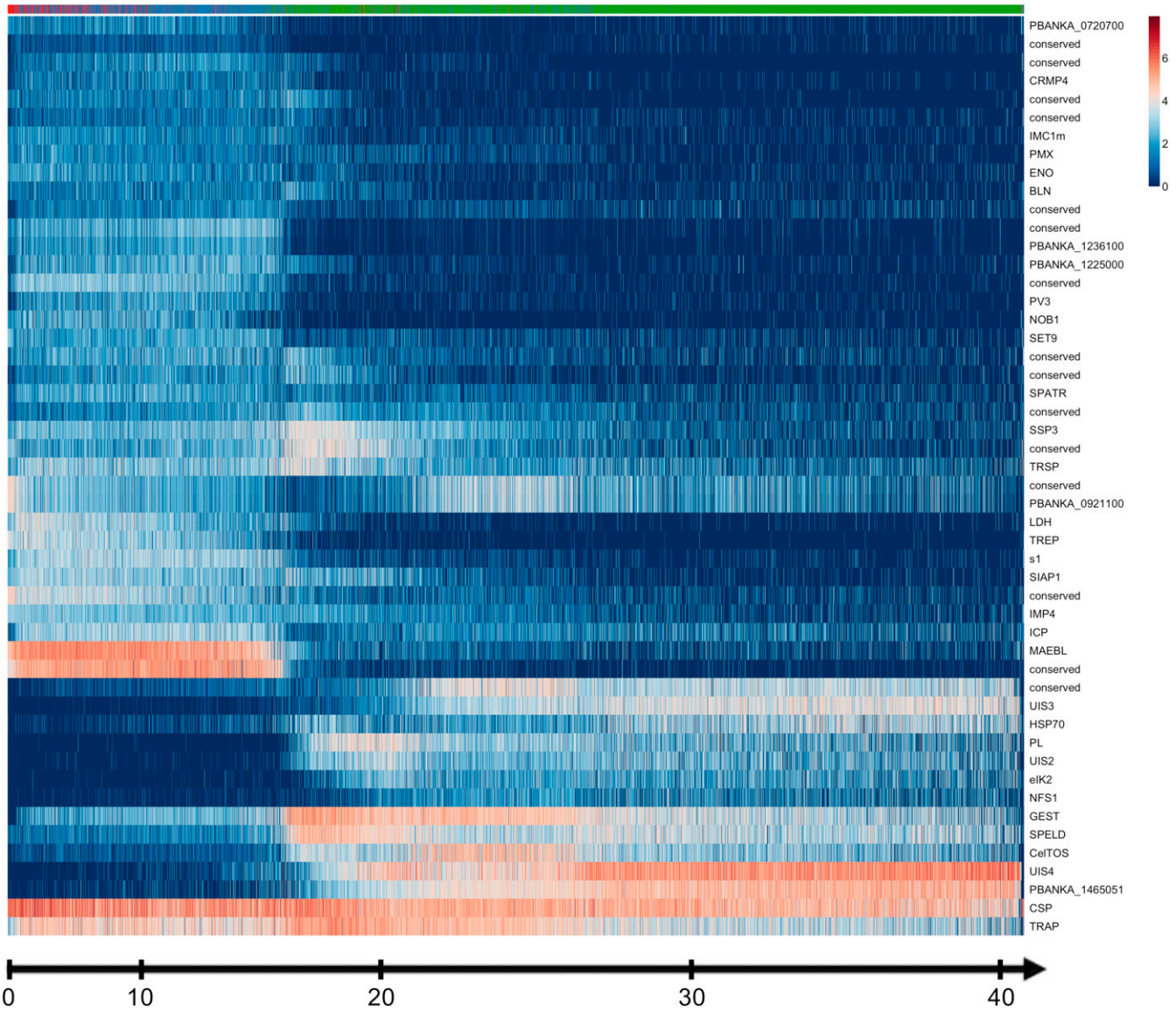

Fig. 2. Heatmap showing the expression patterns for the 50 most differentially expressed genes during sporozoite development in mosquitoes (from oocyst to mature salivary gland sporozoites). Each row shows the expression of one protein-coding gene. Each column shows the data for one individual sporozoite, organized from left to right according to its pseudotime and colored by its anatomical location in the track above the heatmap (red, oocyst; blue, hemolymph; and green, salivary gland). The heatmap color shows the number of a given transcript per cell from dark blue (not detected) to white and red (most highly expressed). The black arrow at the bottom indicates the corresponding pseudotimes.

(rRNA) molecules synthesized in sporozoites collected by forced salivation compared to the amount observed in oocyst to salivary gland sporozoites (Fig. 4*B*). While rRNA molecules are not polyadenylated in *Plasmodium* and should theoretically not pass the polyA selection used during the 10× scRNA-seq library preparation, they are extremely abundant in cells and are often detected in transcriptomic experiments. Indeed, we observed very specific and consistent expression of the 5.8S, 18S, and 28S rRNA genes (*SI Appendix*, Fig. S6) across the entirety of sporozoite development, with a clear increase upon salivation. This observation would be consistent with the abrupt reactivation of quiescent sporozoites and the restarting of the entire transcriptional/translational machinery upon salivation. In contrast to multicellular eukaryotes that typically have hundreds of copies of rRNA genes in their genome, most *Plasmodium* parasites only carry four copies of the 18S–5.8S–28S ribosomal unit and the expression of these rRNA genes is developmentally regulated (67, 68): The rRNA genes located on *P. berghei* chromosomes 5 and 6 are primarily expressed in mosquito stages (S-forms), while the rRNA genes from chromosomes 7 and 12 are the dominant forms in blood stages (A-forms). Analyses of the rRNA sequences that carried sufficient genetic information to reliably differentiate the chromosomal origin of each rRNA transcript (*Materials and Methods*) indicated that there were approximately twice as many transcripts derived from chromosome 6 (S-form) than the combined number of transcripts derived from chromosomes 7 and 12 (A-forms), while no transcripts specifically derived from chromosome 5 (also S-form) could be detected in our data (*SI Appendix*, Fig. S7). Interestingly, the A/S proportions remained relatively constant throughout sporozoite development and, in particular, did not change upon salivation, suggesting that the switch to the A-form rRNAs observed in blood-stage parasites occurs at some point during the liver stage development.

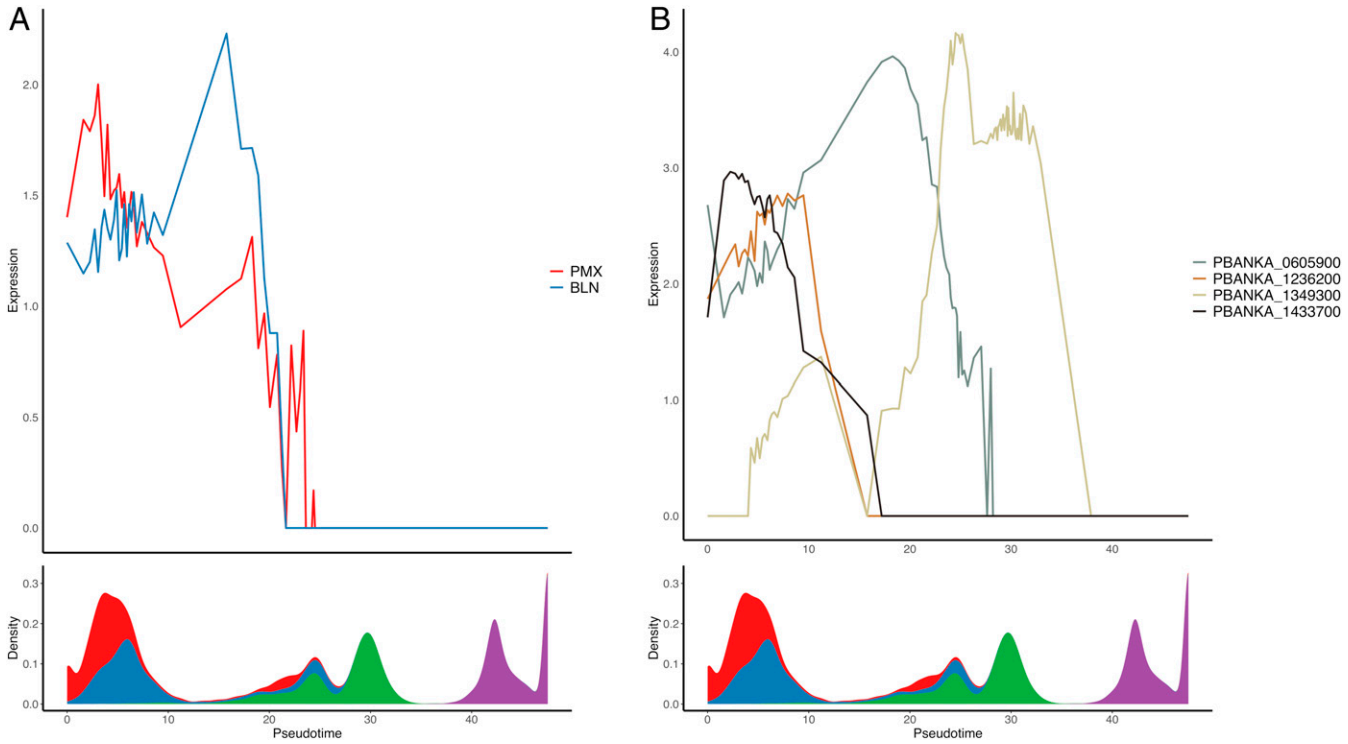

Fig. 3. Novel candidate genes that could play a role in sporozoite development. (*A*) Changes in expression of Plasmepsin-X (PMX, red) and Bergheilysin (BLN, blue) during sporozoite development. (*B*) Changes of expression of five conserved unannotated *P. berghei* genes with distinct expression patterns throughout sporozoite development. Each plot shows the median gene expression of 100 individual parasites (*y* axis) binned according to their pseudotime (*x* axis). The plot under each graph summarizes the distribution of the pseudotimes obtained for oocyst (red), hemolymph (blue), salivary gland (green), and salivated (purple) sporozoites.

Conclusion

Our data provide a comprehensive perspective on the regulation of gene expression accompanying the development of *P. berghei* sporozoites from midgut oocyst to mature salivary gland sporozoites, and upon salivation. The single-cell analyses reveal a high level of transcriptional heterogeneity among sporozoites from the same anatomical location, which was masked in previous gene expression studies. This transcriptional heterogeneity possibly derives from the asynchronicity of oocyst maturation and sporozoite egress, and indicates that the development of *Plasmodium* parasites in mosquitoes is, at least partially, regulated by an intrinsic clock and not solely determined by the parasite environment. The data generated also highlight the key role of transcriptional regulation in the quiescence and reactivation of salivary gland sporozoites: The genes underlying the global translational repression in mature parasites are specifically transcribed once the sporozoites reach the salivary glands and this transcription is accompanied by a general decrease in transcriptional activity, while, upon salivation, the increase in the level of rRNA genes is consistent with a restarting of the entire transcriptional machinery.

The precise determination of the timing of expression of each *P. berghei* gene may enable the identification of novel candidate genes that underlie specific biological processes (e.g., oocyst egress or invasion of salivary gland cells) and improve our understanding of the regulation of these functions in sporozoites. In addition, this study can constitute a framework to identify and manipulate critical determinants of sporozoite development and transmission to mammalian hosts and serve as a foundation for developing new strategies to malaria control.

Materials and Methods

Parasite and Mosquito Strains. Infections of *An. stephensi* mosquitoes [Nijmegen strain (69)] were performed with *P. berghei* ANKA parasites expressing the green fluorescent protein (GFP) ($PbGFP_{CON}$) (70) at the insectary of the Laboratory for Malaria and Vector Research of the National Institute of Allergy and Infectious Diseases (NIAID)/NIH. Infections of *An. stephensi* mosquitoes (Liston strain) were performed with *P. berghei* ANKA line 159cl1 that constitutively expresses mCherry (54) at the Johns Hopkins Bloomberg School of Public Health.

An. stephensi mosquitoes were reared under standard insectary conditions at 80% humidity, 12/12-h light/dark cycle, and maintained with cotton pads soaked either in 10% sucrose solution or 10% corn syrup solution (Karo; ACH Food Companies).

Animal Handling and Ethics Protocol. This study was performed following the recommendations from the *Guide for the Care and Use of Laboratory Animals* of the NIH (71). The animal use was approved by the Johns Hopkins Institutional Biosafety Committee and Johns Hopkins University Institutional Animal Care and Use Committee (MO17H325), and by the NIH Animal Ethics Proposal and registered in the Standard Operating Procedures of Laboratory of Malaria and Vector Research (NIAID/NIH-SOP LMVR 22).

Infection Conditions. Three- to 4-wk-old Swiss-Webster mice were infected with *P. berghei* from frozen stocks, and the mouse parasitemia was monitored daily by light microscopy analysis of methanol-fixed blood smear stained with 10% Giemsa. Four- to 5-d-old *An. stephensi* females were starved for 12 h before being allowed to feed for 30 min on an anesthetized mouse infected with *P. berghei* with ~1% parasitemia and an exflagellation rate of 1:10 fields. Only fully engorged mosquitoes were kept and maintained at 18 °C (Johns Hopkins Bloomberg School of Public Health) or 19 °C (NIAID) with 10% sugar solution ad libitum until sporozoite collection.

Isolation of *P. berghei*-GFP Sporozoites. To isolate sporozoites from oocysts, 50 female mosquitoes were dissected 14 d after the infected blood meal. Mosquitoes were anesthetized on ice and the midguts were dissected under a stereomicroscope in phosphate-buffered saline (PBS). The midguts were placed in an excavated Petri dish with PBS under a fluorescent microscope, opened, and the oocysts were disrupted with a needle to release the sporozoites. The released sporozoites were collected with a Sigmacote-coated

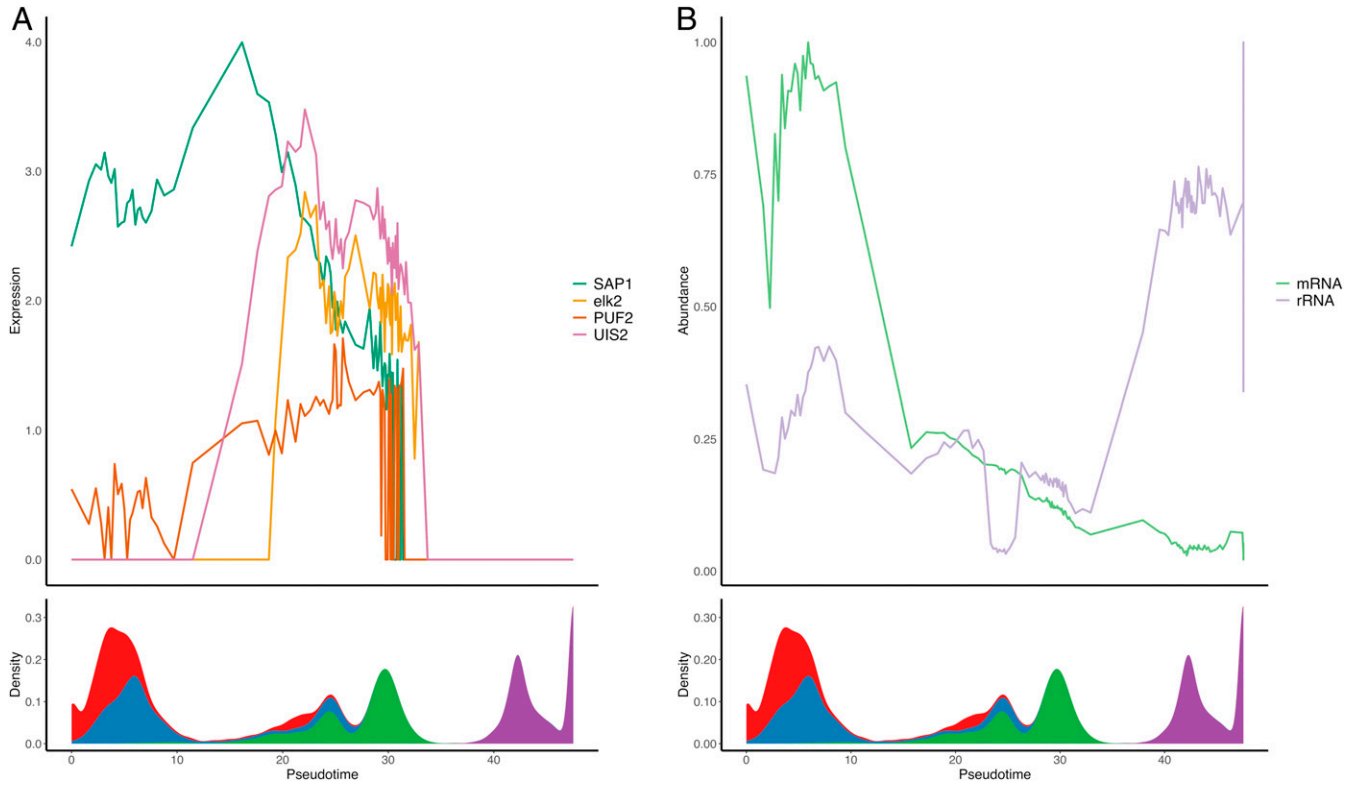

Fig. 4. Regulation of transcription and translation in sporozoite. (*A*) Changes in expression of *Plasmodium* genes involved in mRNA stability (SAP1, green) and translation inhibition (eIK2, orange; PUF2, red; UIS2, pink). (*B*) Changes in relative abundance of mRNA (green) and rRNAs (purple) during sporozoite development. Both the mRNA and rRNA curves show the proportion of RNA at a given pseudotime compared to the maximum observed (fixed arbitrarily at 1). The plot under each graph summarizes the distribution of the pseudotimes obtained for oocyst (red), hemolymph (blue), salivary gland (green), and salivated (purple) sporozoites.

pipette tip (Sigma) and transferred to a low-retention tube (Protein LoBind; Eppendorf).

Hemolymph sporozoites were collected by perfusion of 50 ice-cold anesthetized females at day 16 postinfection. Mosquitoes were gradually injected with 10 μL of PBS into the thorax, and the sporozoites were collected from the flow-through by an incision made in the abdominal wall using forceps. The samples were collected with a Sigmacote-coated tip and transferred to a low-retention tube (Protein LoBind Tube; Eppendorf) on ice.

Sporozoites from salivary glands were collected at 21 dpi. One day before sporozoite collection, salivary gland infection was confirmed by the accumulation of parasite-expressed GFP on the mosquito thoracic cavity under a fluorescent microscope (MZ10 F; Leica). Fifty female mosquitoes were anesthetized on ice and their salivary glands dissected in PBS under a stereomicroscope. The salivary glands were transferred to a low-retention tube (Protein LoBind Tube; Eppendorf) containing PBS, homogenized with a disposable pestle, and kept on ice.

Salivated sporozoites were collected from 60 infected female mosquitoes at day 21 postinfection by forced probing in a Sigmacote-coated tip filled with 10 μL of PBS. Briefly, mosquitoes were anesthetized on ice for 5 min, the wings were removed, and the mosquito proboscis was gently inserted into the tip. The mosquitoes were left to salivate for 30 min, and the salivated sporozoites were pooled in a low-retention tube (Protein LoBind Tube; Eppendorf). After collection, all the samples were homogenized, passed through a 20-μm Pluriselect filter (Cell Strainer) to remove cellular debris, and counted using a hemocytometer (C-Chip; Chemglass Life Sciences). The excess volume was removed by centrifugation at 15,000 × *g* for 10 min, and the sporozoite final concentration adjusted to 500 to 2,000 sporozoites per microliter in PBS.

Isolation of *P. berghei*-mCherry Sporozoites from Mosquito Saliva and Salivary Glands. One day prior to sporozoite collection, mosquitoes were fluorescently sorted and mosquitoes with fluorescence in the salivary gland area were kept for sporozoite harvest. Salivary gland and salivated sporozoites were collected from mosquitoes 21 or 22 dpi. Briefly, mosquitoes were anesthetized on ice for 5 min and immobilized on a glass plate by placing their wings on double-sided tape. The mosquito proboscis was gently inserted into a low-adhesion P10 pipet tip containing 2 μL of immersion oil (ZEISS; Immersol 518F) or 4 μL of PBS. Salivation was induced by applying 1% pilocarpine (Sigma; P6503)/0.2% Tween 20 (Sigma; P1379) in PBS to the mosquito abdomen. Following this, mosquitoes were allowed to salivate for 30 min. Salivated sporozoites were collected from 60 to 78 mosquitoes by pooling pipet tips containing saliva sporozoites in a low-retention 0.6-mL tube (Thermo Fisher; 3446). For sporozoites salivated into oil collection, pooled oil was mixed with 20 μL of PBS and spun at 1,000 × *g* for 5 min to separate saliva from oil.

Library Preparation and Sequencing. The number of sporozoites isolated from each sample was crudely determined using a hemocytometer and light microscopy. An estimated 1,000 to 5,000 sporozoites per sample were loaded on a 10× Genomics Chromium controller and 12 individually barcoded 3′-end scRNA-seq libraries were prepared according to the manufacturer's protocol. Briefly, the 10× 3′-end library preparation includes physical isolation of individual cells in droplets, capture of the polyadenylated mRNAs using oligo-dT priming, and reverse transcription incorporating a barcode specific to each droplet (37). After cDNA synthesis, the emulsion is broken and cDNA molecules are fragmented into ~300-bp fragments, before the addition of sequencing adapters. Each library was sequenced on an Illumina high-output sequencer to generate a total of 2,296,539,124 75-bp paired-end reads (*SI Appendix*, Table S1).

Single-Cell Transcriptome Analysis. A custom analysis pipeline, similar to the Cell Ranger single-cell software (37), was developed to process all scRNA-seq reads (32). Briefly, we identified all reads containing the 10× Genomics barcodes, trimmed of sequences downstream of 3′ polyadenylation tails, and only kept for further analyses reads longer than 40 bp. We mapped all reads using HISAT2 [version 2.0.4 (72)] to the *P. berghei* ANKA genome (38), allowing for a maximum intron length of 5,000 bp, and to the *An. stephensi* genome [AsteS1 (73)]. To identify sequences that represent PCR duplicates resulting from the library preparation, we identified reads with identical sequences for the 16-mer 10× Genomics barcode, 12-mer unique molecular identifier sequence,

and mapped to the same genomic location of DNA and on the same strand, and only kept one of them. These "unique reads," of which each represents a unique mRNA molecule present in one parasite, were then further analyzed. We used the 10× Genomics barcodes to assign unique reads to individual parasites and tallied the number of unique reads mapped to each annotated *P. berghei* gene (i.e., from the annotated transcription start site to 500 bp after the 3′-end).

We then combined all scRNA-seq libraries and used the scran [v1.14.6 (74)] addPerCellQC function to identify and remove outlier cells based on library size and gene count while accounting for variations between libraries (e.g., sequencing depth). Only transcriptomes with more than 200 unique reads were included. Transcripts detected in less than 300 cells (out of 16,038) were excluded from this analysis. We normalized the transcriptomes of these filtered transcriptomes and calculated size factors by deconvolution using the scran functions quickCluster and computeSumFactors. The calculated size factors were used to compute normalized counts per cell via logNormCounts function in scater (v1.14.6) (75) and performed PCA with runPCA. In addition, to evaluate the effect of cells characterized by a small number of unique reads, we reran this analysis using only transcriptomes characterized by at least 1,000 unique reads.

Estimation of the Pseudotime and Differential Expression Analysis. The dataset analyzed with scran/scatter—raw counts, normalized counts, reduced dimensionality (PCA), and metadata—was then imported to slingshot (v1.4.0) (39) to calculate pseudotime for all individual parasites.

To identify genes that were differentially expressed along the estimated pseudotime trajectory, we used the fitGAM function ($k = 7$) of tradeSeq [v1.1.19 (76)]. Due to the low mRNA transcript abundance observed in salivated sporozoites, we performed the statistical testing separately with and without data from these experiments (i.e., using only data from sporozoites collected from oocyst, hemolymph, and salivary gland; or using the entire dataset). We tested for differentially expressed genes according to the calculated trajectory using the associationTest function and corrected *P* values for multiple testing using false discovery rates (77, 78).

Analysis of rRNA Genes. All scRNA-seq reads were also mapped independently to the four chromosomal locations of the *P. berghei* genome containing the 18S–5.8S–28S rRNA genes (on chromosomes 5, 6, 7, and 12) using Hisat2 but without allowing for spliced alignments (–no-spliced-alignment mode) to avoid mismapping caused by the high sequence homology among loci. Very few reads mapped to the 5S rRNA gene cluster on chromosome 10, and those were not included in these analyses. We tallied the number of reads unambiguously mapped to each chromosomal location for each individual parasite. To control for variations in the number of informative reads derived from each chromosome, we split the reference sequence of each rRNA genes into 75 bp (with a shift of 1 bp) and determined the proportion of reads, from each gene, mapped unambiguously to its original location.

Data Availability. All sequence data generated in this study have been deposited in the National Center for Biotechnology Information (NCBI) Sequence Read Archive under the BioProject ID PRJNA676126.

ACKNOWLEDGMENTS. We thank S. Ott, H. Bowen, L. Sadzewicz, and L. Tallon in the Genomic Resource Center at the University of Maryland School of Medicine for their support with 10X library preparation and Illumina sequencing. We also thank Godfree Mlambo, Abhai Tripathi, and Chris Kizito for their exceptional support in rearing and infecting mosquitoes at Johns Hopkins University. This work was supported by awards from the NIH to the University of Maryland School of Medicine (R21 AI143932 and U19 AI110820) and Johns Hopkins Bloomberg School of Public Health (R01 AI132359), by the Intramural Research Program of the National Institute of Allergy and Infectious Diseases, NIH, and by Bloomberg Philanthropies. The funders had no role in study design, data collection and analysis, decision to publish, or preparation of the manuscript.

1. L. S. Tusting *et al*., Socioeconomic development as an intervention against malaria: A systematic review and meta-analysis. *Lancet* **382**, 963–972 (2013).
2. J. Utzinger, M. Tanner, Socioeconomic development to fight malaria, and beyond. *Lancet* **382**, 920–922 (2013).
3. S. Q. Wang *et al*., Prevention measures and socio-economic development result in a decrease in malaria in Hainan, China. *Malar. J.* **13**, 362 (2014).
4. malERA Consultative Group on Health Systems and Operational Research, A research agenda for malaria eradication: Health systems and operational research. *PLoS Med.* **8**, e1000397 (2011).
5. S. Bhatt *et al*., The effect of malaria control on *Plasmodium falciparum* in Africa between 2000 and 2015. *Nature* **526**, 207–211 (2015).
6. malERA Consultative Group on Vector Control, A research agenda for malaria eradication: Vector control. *PLoS Med.* **8**, e1000401 (2011).
7. T. N. Wells, R. Hooft van Huijsduijnen, W. C. Van Voorhis, Malaria medicines: A glass half full? *Nat. Rev. Drug Discov.* **14**, 424–442 (2015).
8. J. N. Burrows *et al*., New developments in anti-malarial target candidate and product profiles. *Malar. J.* **16**, 26 (2017).
9. World Health Organization, World malaria report 2019. https://www.who.int/publications/i/item/9789241565721. Accessed 18 February 2020.
10. P. Adepoju, RTS,S malaria vaccine pilots in three African countries. *Lancet* **393**, 1685 (2019).
11. RTS,S Clinical Trials Partnership, Efficacy and safety of RTS,S/AS01 malaria vaccine with or without a booster dose in infants and children in Africa: Final results of a phase 3, individually randomised, controlled trial. *Lancet* **386**, 31–45 (2015).
12. M. S. Sissoko *et al*., Safety and efficacy of PfSPZ vaccine against *Plasmodium falciparum* via direct venous inoculation in healthy malaria-exposed adults in Mali: A randomised, double-blind phase 1 trial. *Lancet Infect. Dis.* **17**, 498–509 (2017).
13. M. Roestenberg *et al*., A double-blind, placebo-controlled phase 1/2a trial of the genetically attenuated malaria vaccine PfSPZ-GA1. *Sci. Transl. Med.* **12**, eaaz5629 (2020).
14. K. E. Lyke *et al*.; Warfighter II Study Team, Multidose priming and delayed boosting improve PfSPZ vaccine efficacy against heterologous *P. falciparum* controlled human malaria infection. *Clin. Infect. Dis.*, 10.1093/cid/ciaa1294 (2020).
15. R. J. Porter, R. L. Laird, E. M. Dusseau, Studies on malarial sporozoites. II. Effect of age and dosage of sporozoites on their infectiousness. *Exp. Parasitol.* **3**, 267–274 (1954).
16. W. Graumans, E. Jacobs, T. Bousema, P. Sinnis, When is a *Plasmodium*-infected mosquito an infectious mosquito? *Trends Parasitol.* **36**, 705–716 (2020).
17. D. L. Medica, P. Sinnis, Quantitative dynamics of *Plasmodium yoelii* sporozoite transmission by infected anopheline mosquitoes. *Infect. Immun.* **73**, 4363–4369 (2005).
18. J. P. Vanderberg, Development of infectivity by the *Plasmodium berghei* sporozoite. *J. Parasitol.* **61**, 43–50 (1975).
19. Y. Sato, G. N. Montagna, K. Matuschewski, *Plasmodium berghei* sporozoites acquire virulence and immunogenicity during mosquito hemocoel transit. *Infect. Immun.* **82**, 1164–1172 (2014).
20. P. G. Shute, Successful transmission of human malaria with sporozoites which have not come into contact with the salivary glands of the insect host. *J. Trop. Med. Hyg.* **46**, 57–58 (1943).
21. M. G. Touray, A. Warburg, A. Laughinghouse, A. U. Krettli, L. H. Miller, Developmentally regulated infectivity of malaria sporozoites for mosquito salivary glands and the vertebrate host. *J. Exp. Med.* **175**, 1607–1612 (1992).
22. S. A. Mikolajczak *et al*., Distinct malaria parasite sporozoites reveal transcriptional changes that cause differential tissue infection competence in the mosquito vector and mammalian host. *Mol. Cell. Biol.* **28**, 6196–6207 (2008).
23. S. E. Lindner *et al*., Transcriptomics and proteomics reveal two waves of translational repression during the maturation of malaria parasite sporozoites. *Nat. Commun.* **10**, 4964 (2019).
24. A. S. Aly, K. Matuschewski, A malarial cysteine protease is necessary for *Plasmodium* sporozoite egress from oocysts. *J. Exp. Med.* **202**, 225–230 (2005).
25. S. Engelmann, O. Silvie, K. Matuschewski, Disruption of *Plasmodium* sporozoite transmission by depletion of sporozoite invasion-associated protein 1. *Eukaryot. Cell* **8**, 640–648 (2009).
26. B. Douradinha *et al*., *Plasmodium* cysteine repeat modular proteins 3 and 4 are essential for malaria parasite transmission from the mosquito to the host. *Malar. J.* **10**, 71 (2011).
27. A. Combe *et al*., TREP, a novel protein necessary for gliding motility of the malaria sporozoite. *Int. J. Parasitol.* **39**, 489–496 (2009).
28. T. Kariu, M. Yuda, K. Yano, Y. Chinzei, MAEBL is essential for malarial sporozoite infection of the mosquito salivary gland. *J. Exp. Med.* **195**, 1317–1323 (2002).
29. J. M. Myung, P. Marshall, P. Sinnis, The *Plasmodium* circumsporozoite protein is involved in mosquito salivary gland invasion by sporozoites. *Mol. Biochem. Parasitol.* **133**, 53–59 (2004).
30. A. Poran *et al*., Single-cell RNA sequencing reveals a signature of sexual commitment in malaria parasites. *Nature* **551**, 95–99 (2017).
31. A. J. Reid *et al*., Single-cell RNA-seq reveals hidden transcriptional variation in malaria parasites. *eLife* **7**, e33105 (2018).
32. J. M. Sà, M. V. Cannon, R. L. Caleon, T. E. Wellems, D. Serre, Single-cell transcription analysis of *Plasmodium vivax* blood-stage parasites identifies stage- and species-specific profiles of expression. *PLoS Biol.* **18**, e3000711 (2020).
33. V. M. Howick *et al*., The Malaria Cell Atlas: Single parasite transcriptomes across the complete *Plasmodium* life cycle. *Science* **365**, eaaw2619 (2019).
34. E. Bushell *et al*., Functional profiling of a *Plasmodium* genome reveals an abundance of essential genes. *Cell* **170**, 260–272.e8 (2017).
35. A. R. Gomes *et al*., A genome-scale vector resource enables high-throughput reverse genetic screening in a malaria parasite. *Cell Host Microbe* **17**, 404–413 (2015).
36. R. R. Stanway *et al*., Genome-scale identification of essential metabolic processes for targeting the *Plasmodium* liver stage. *Cell* **179**, 1112–1128.e26 (2019).
37. G. X. Zheng *et al*., Massively parallel digital transcriptional profiling of single cells. *Nat. Commun.* **8**, 14049 (2017).

38. A. Fougère *et al*., Variant exported blood-stage proteins encoded by *Plasmodium* multigene families are expressed in liver stages where they are exported into the parasitophorous vacuole. *PLoS Pathog.* **12**, e1005917 (2016).
39. K. Street *et al*., Slingshot: Cell lineage and pseudotime inference for single-cell transcriptomics. *BMC Genomics* **19**, 477 (2018).
40. K. Matuschewski *et al*., Infectivity-associated changes in the transcriptional repertoire of the malaria parasite sporozoite stage. *J. Biol. Chem.* **277**, 41948–41953 (2002).
41. G. Costa *et al*., Non-competitive resource exploitation within mosquito shapes within-host malaria infectivity and virulence. *Nat. Commun.* **9**, 3474 (2018).
42. A. Harupa *et al*., SSP3 is a novel *Plasmodium yoelii* sporozoite surface protein with a role in gliding motility. *Infect. Immun.* **82**, 4643–4653 (2014).
43. K. E. Boysen, K. Matuschewski, Inhibitor of cysteine proteases is critical for motility and infectivity of *Plasmodium* sporozoites. *MBio* **4**, e00874-13 (2013).
44. A. K. Mueller *et al*., *Plasmodium* liver stage developmental arrest by depletion of a protein at the parasite-host interface. *Proc. Natl. Acad. Sci. U.S.A.* **102**, 3022–3027 (2005).
45. A. K. Mueller, M. Labaied, S. H. Kappe, K. Matuschewski, Genetically modified *Plasmodium* parasites as a protective experimental malaria vaccine. *Nature* **433**, 164–167 (2005).
46. T. Kariu, T. Ishino, K. Yano, Y. Chinzei, M. Yuda, CelTOS, a novel malarial protein that mediates transmission to mosquito and vertebrate hosts. *Mol. Microbiol.* **59**, 1369–1379 (2006).
47. M. Zhang, S. Mishra, R. Sakthivel, B. M. Fontoura, V. Nussenzweig, UIS2: A unique phosphatase required for the development of *Plasmodium* liver stages. *PLoS Pathog.* **12**, e1005370 (2016).
48. M. Labaied, N. Camargo, S. H. Kappe, Depletion of the *Plasmodium berghei* thrombospondin-related sporozoite protein reveals a role in host cell entry by sporozoites. *Mol. Biochem. Parasitol.* **153**, 158–166 (2007).
49. A. M. Talman *et al*., PbGEST mediates malaria transmission to both mosquito and vertebrate host. *Mol. Microbiol.* **82**, 462–474 (2011).
50. P. Bhanot, K. Schauer, I. Coppens, V. Nussenzweig, A surface phospholipase is involved in the migration of *Plasmodium* sporozoites through cells. *J. Biol. Chem.* **280**, 6752–6760 (2005).
51. A. Coppi *et al*., The malaria circumsporozoite protein has two functional domains, each with distinct roles as sporozoites journey from mosquito to mammalian host. *J. Exp. Med.* **208**, 341–356 (2011).
52. A. A. Sultan *et al*., TRAP is necessary for gliding motility and infectivity of plasmodium sporozoites. *Cell* **90**, 511–522 (1997).
53. A. S. Nasamu *et al*., Plasmepsins IX and X are essential and druggable mediators of malaria parasite egress and invasion. *Science* **358**, 518–522 (2017).
54. C. S. Hopp *et al*., Longitudinal analysis of *Plasmodium* sporozoite motility in the dermis reveals component of blood vessel recognition. *eLife* **4**, e07789 (2015).
55. M. Zhang *et al*., The *Plasmodium* eukaryotic initiation factor-2alpha kinase IK2 controls the latency of sporozoites in the mosquito salivary glands. *J. Exp. Med.* **207**, 1465–1474 (2010).
56. L. Cui, S. Lindner, J. Miao, Translational regulation during stage transitions in malaria parasites. *Ann. N. Y. Acad. Sci.* **1342**, 1–9 (2015).
57. S. S. Vembar, D. Droll, A. Scherf, Translational regulation in blood stages of the malaria parasite *Plasmodium* spp.: Systems-wide studies pave the way. *Wiley Interdiscip. Rev. RNA* **7**, 772–792 (2016).
58. K. T. Rios, S. E. Lindner, Protein-RNA interactions important for *Plasmodium* transmission. *PLoS Pathog.* **15**, e1008095 (2019).
59. O. Turque, T. Tsao, T. Li, M. Zhang, Translational repression in malaria sporozoites. *Microb. Cell* **3**, 227–229 (2016).
60. S. Bennink, G. Pradel, The molecular machinery of translational control in malaria parasites. *Mol. Microbiol.* **112**, 1658–1673 (2019).
61. G. R. Mair *et al*., Regulation of sexual development of *Plasmodium* by translational repression. *Science* **313**, 667–669 (2006).
62. S. Jain *et al*., ATPase-modulated stress granules contain a diverse proteome and substructure. *Cell* **164**, 487–498 (2016).
63. A. S. Aly, S. E. Lindner, D. C. MacKellar, X. Peng, S. H. Kappe, SAP1 is a critical post-transcriptional regulator of infectivity in malaria parasite sporozoite stages. *Mol. Microbiol.* **79**, 929–939 (2011).
64. A. S. Aly *et al*., Targeted deletion of SAP1 abolishes the expression of infectivity factors necessary for successful malaria parasite liver infection. *Mol. Microbiol.* **69**, 152–163 (2008).
65. H. J. Painter, M. Carrasquilla, M. Llinás, Capturing in vivo RNA transcriptional dynamics from the malaria parasite *Plasmodium falciparum*. *Genome Res.* **27**, 1074–1086 (2017).
66. H. J. Painter *et al*., Genome-wide real-time in vivo transcriptional dynamics during *Plasmodium falciparum* blood-stage development. *Nat. Commun.* **9**, 2656 (2018).
67. A. P. Waters, C. Syin, T. F. McCutchan, Developmental regulation of stage-specific ribosome populations in *Plasmodium*. *Nature* **342**, 438–440 (1989).
68. J. Thompson *et al*., Heterogeneous ribosome populations are present in *Plasmodium berghei* during development in its vector. *Mol. Microbiol.* **31**, 253–260 (1999).
69. A. M. Feldmann, T. Ponnudurai, Selection of *Anopheles stephensi* for refractoriness and susceptibility to *Plasmodium falciparum*. *Med. Vet. Entomol.* **3**, 41–52 (1989).
70. B. Franke-Fayard *et al*., A *Plasmodium berghei* reference line that constitutively expresses GFP at a high level throughout the complete life cycle. *Mol. Biochem. Parasitol.* **137**, 23–33 (2004).
71. National Research Council, *Guide for the Care and Use of Laboratory Animals (National Academies Press*, Washington, DC, ed. 8, 2011).
72. D. Kim, B. Langmead, S. L. Salzberg, HISAT: A fast spliced aligner with low memory requirements. *Nat. Methods* **12**, 357–360 (2015).
73. D. E. Neafsey *et al*., Mosquito genomics. Highly evolvable malaria vectors: The genomes of 16 *Anopheles* mosquitoes. *Science* **347**, 1258522 (2015).
74. A. T. Lun, K. Bach, J. C. Marioni, Pooling across cells to normalize single-cell RNA sequencing data with many zero counts. *Genome Biol.* **17**, 75 (2016).
75. A. T. Lun, D. J. McCarthy, J. C. Marioni, A step-by-step workflow for low-level analysis of single-cell RNA-seq data with Bioconductor. *F1000 Res.* **5**, 2122 (2016).
76. K. Van den Berge *et al*., Trajectory-based differential expression analysis for single-cell sequencing data. *Nat. Commun.* **11**, 1201 (2020).
77. Y. Benjamini, Y. Hochberg, Controlling the false discovery rate: A practical and powerful approach to multiple testing. *J. R. Stat. Soc. B* **57**, 289–300 (1995).
78. J. D. Storey, R. Tibshirani, Statistical significance for genomewide studies. *Proc. Natl. Acad. Sci. U.S.A.* **100**, 9440–9445 (2003).
79. J. Togiri *et al*., Plasmodium berghei sporozoite specific genes- PbS10 and PbS23/SSP3 are required for the development of exo-erythrocytic forms. *Mol. Biochem. Parasitol.* **232**, 111198 (2019).
80. D. K. Jaijyan, P. K. Verma, A. P. Singh, A novel FIKK kinase regulates the development of mosquito and liver stages of the malaria. *Sci. Rep.* **6**, 39285 (2016).
81. C. Lehmann *et al*., A cysteine protease inhibitor of plasmodium berghei is essential for exo-erythrocytic development. *PLoS Pathog.* **10**, e1004336 (2014).
82. R. Ménard *et al*., Circumsporozoite protein is required for development of malaria sporozoites in mosquitoes. *Nature* **385**, 336–340 (1997).